Diphenyl Phosphonate Inhibitors for the Urokinase-Type Plasminogen Activator: Optimization of the P4 Position

Jurgen Joossens,[†] Pieter Van der Veken,[†] Georgiana Surpateanu,[†] Anne-Marie Lambeir,[‡] Ibrahim El-Sayed,[†] Omar M. Ali,[†] Koen Augustyns,*[,†] and Achiel Haemers[†]

Laboratory of Medicinal Chemistry and Laboratory of Medical Biochemistry, University of Antwerp, Universiteitsplein 1, BE-2610 Antwerp, Belgium

Received May 24, 2006

This paper describes the structure−activity relationship in a series of tripeptidyl diphenyl phosphonate irreversible urokinase plasminogen activator (uPA) inhibitors, originally derived from an arginyltripeptide. uPA is considered an interesting target in anticancer drug design. The selectivity of these inhibitors for uPA is enhanced by the optimization of the P4 position. The most interesting compound shows an IC_{50} of 5 nM, with a selectivity index of more than 3000 toward other Arg/Lys-specific proteases such as tissue-type plasminogen activator, plasmin, factor Xa, and thrombin. A synthetic strategy for the preparation of small libraries of diphenyl phosphonate analogues of capped tripeptides is described. It is shown that uPA is irreversibly inhibited, and interactions with the active site were modeled. Finally, a diparacetamol phosphonate analogue was developed to circumvent the release of cytotoxic phenol.

Introduction

Urokinase plasminogen activator (uPA)[a] is a trypsin-like serine protease and a pivotal enzyme in pericellular proteolysis. It is produced as a pro-enzyme, pro-uPA, and activated by plasmin and some other proteases. It is selectively bound to its membrane-anchored receptor (uPAR) and activates plasminogen into plasmin. Plasmin plays an important role in the breakdown of extracellular matrix (ECM). It activates several matrix metalloproteases, which in turn degrade several components of the ECM including fibrin, laminin, and fibronectin. Proteolytic degradation of this ECM is very important for tumor growth and metastasis, and the uPA−uPAR system appears to be a key player in the proteolytic degradation process in cancer invasion and metastasis. Although proteolysis during cancer progession is a very complex event, it becomes more and more evident that plasminogen activation by uPA and the uPA−uPAR[1−3] complex, together with other extracellular proteases,[4] may be an attractive target in the discovery of new antimetastasis approaches.

Some recent data support uPA/uPAR as a valid therapeutic target. A small synthetic amidinophenylalanine-type uPA inhibitor (WX-UK1) suppresses rat breast cancer metastasis and reduces primary tumor growth. This inhibitor is currently in phase I/II trials.[5] Another amidine-based, peptide-derived inhibitor reduces the number of experimental lung metastasis in a fibrosarcoma model in mice.[6] uPA-deficient mice show reduced metastasis of transgenic mammary cancer.[7] Down regulation of uPAR suppresses invasiveness in colon cancer cells.[8] Antisense oligonucleotides for uPAR inhibit metastasis of human melanoma[9] and experimental prostate cancer bone metastases[10] in mice. The uPA and uPAR status is one of the strongest prognostic factors in breast carcinoma.[11]

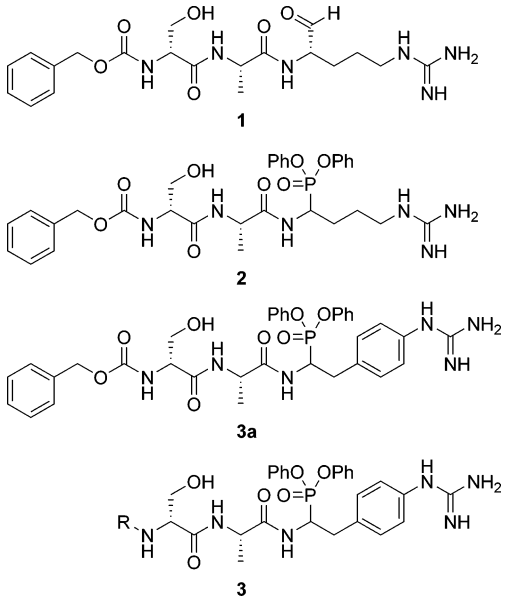

Figure 1. Development of the uPA inhibitors **3** from the peptidic arginal **1** as lead compound.

Moreover, the physiological role of uPA can be taken over by tissue plasminogen activator (tPA). tPA is also able to activate plasminogen but is known to be mainly involved in the fibrinolysis process. The majority of uPA-deficient mice do not develop spontaneous phenotype. This is also true for tPA-deficient mice but not for uPA/tPA- or plasminogen-deficient animals.[6] Hence, we could expect that targeting the uPA system would not lead to mechanism-based toxicity.

Our research focuses on the discovery and development of uPA inhibitors. The development of selective inhibitors for uPA is hampered by its close resemblance to other trypsin-like serine proteases, and several inhibitors suffer from a poor selectivity toward tPA, plasmin, or thrombin. Because the latter enzymes are members of the important blood coagulation cascade, the development of highly selective uPA inhibitors is of utmost importance. The structure of uPA is well-known, and several

* To whom correspondence should be addressed: Tel.: +32-3-8202703. Fax: +32-3-8202739. E-mail: koen.augustyns@ua.ac.be.

[†] Laboratory of Medicinal Chemistry.

[‡] Laboratory of Medical Biochemistry.

[a] Abbreviations: uPA, urokinase-type plasminogen activator; tPA, tissue-type plasminogen activator; uPAR, urokinase-type plasminogen activator receptor; FXa, factor Xa; ECM, extracellular matrix.

10.1021/jm060622g CCC: $33.50
Published on Web 08/24/2006

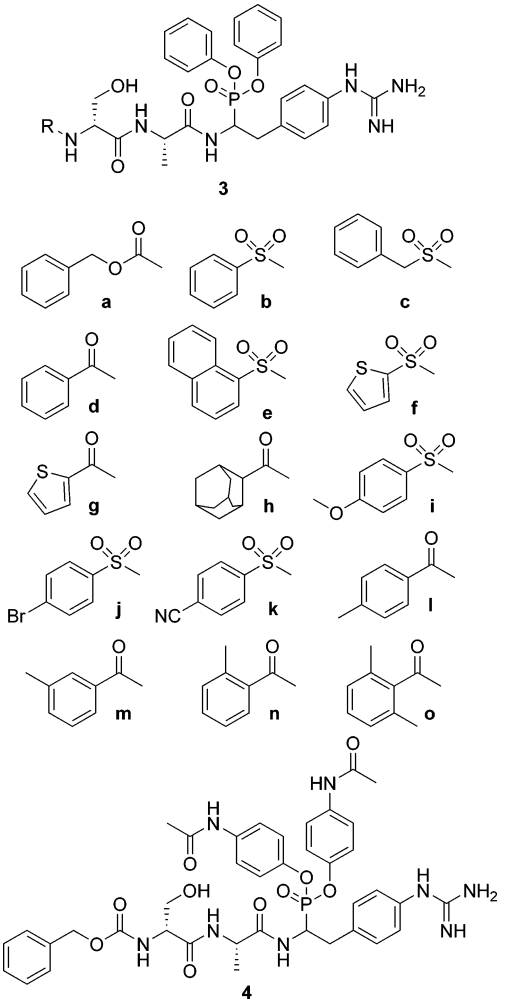

Figure 2. Structures of the diaryl phosphonates reported in this paper.

research groups are involved in the development of reversible inhibitors for uPA. Most of these inhibitors are characterized by a basic function that forms a specific ionic interaction with the carboxylate group of Asp-189 of the S1 site in the deepest pocket of the substrate binding groove of the enzyme.[6,12−14] Peptide as well as nonpeptide inhibitors were developed.

We reported recently the first irreversible, selective and potent diphenyl phosphonate peptidic inhibitors for uPA, based on the *Z*-D-Ser-Ala-Arg structure.[15] These inhibitors were designed using *Z*-D-Ser-Ala-Arginal (**1**) as lead compound (Figure 1).[16] This peptidic compound was derived from a combinatorial library with diversity at P2, P3, and P4. The aldehyde function was replaced by a diphenyl phosphonate group (**2**), which is known to react in a covalent way with the active site serine of serine proteases, affording a phosphonylated and irreversibly inhibited enzyme.[17,18] Because the P1 position was not optimized in the mentioned combinatorial library, we chose to first optimize this position by replacing the arginine moiety by various linear or cyclic guanidinylated side chains. A guanidinylated benzyl group afforded the most interesting compound (**3a)**, providing high selectivity and high potency toward uPA (IC_{50}, 4.3 nM; selectivity toward plasmin, 470; tPA, 1000; thrombin, 4700; trypsin, 70). To the best of our knowledge, these diphenylphosphonate peptides were the first selective and irreversible uPA inhibitors reported in the literature.[15]

In this paper we report the further optimization of this series of phosphonate peptidic inhibitors for uPA (Figure 2). We selected compound **3a** as lead compound and started with the optimization of the P4 postion because it was known from the arginal analogues (**1**) that improvement at this position was possible. We linked several amide (benzamide and substituted benzamides, adamantyl) and sulfonamide (aromatic, benzylic) groups at the terminal amino group (compounds **3b**−**o**) and made a small library of these compounds. Aliphatic groups were not used, as previous investigations, confirmed by literature data,[14,16] showed less convincing results.

Finally, the release of cytotoxic phenol upon covalent binding to the target protein constitutes a potential problem in biological settings using diphenyl phosphonates. To circumvent this problem, a diaryl phosphonate **4** containing a "safe" phenol, *p*-acetylaminophenol (paracetamol), was prepared.

Chemistry

Diphenyl phosphonylated tripeptides were prepared by a fast and convenient synthetic route, affording the opportunity to obtain a diverse series of compounds. The peptide tail of the target compounds was synthesized via standard Fmoc-solid-phase peptide-synthesis protocols (Scheme 1). Using 2-chlorotrityl resin as the solid support, the Fmoc-protected dipeptide (D)-Ser(O*t*-Bu)-Ala **6** was constructed and the N-terminus was capped with different acyl and sulfonyl substituents, affording resin-bound compounds **7**. The capped dipeptide **8** was cleanly cleaved from the resin using dichloromethane/methanol/acetic acid (60:20:20), conditions not affecting the *tert*-butyl protecting group on the serine side chain. The peptide tail was subsequently coupled to the aminophosphonate intermediate **14** by means of a polymer-assisted solution phase procedure, as reported earlier, involving polymer-supported carbodiimide as coupling reagent and a polyamine scavenger resin for purification.[19] The protected compounds **9** were isolated with flash chromatography, and *tert*-butyl and Boc deprotection afforded compounds **3b**−**o**.

Scheme 1. Synthesis of the Target Compounds **3**

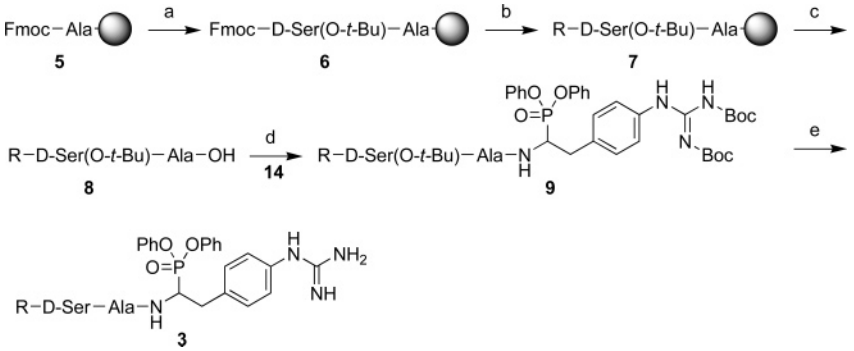

Conditions: (a) (i) piperidine, DMF, (ii) Fmoc-D-Ser(OtBu), TBTU, TEA, DMF; (b) (i) piperidine, DMF, (ii) R′SO_2Cl, collidine, DCM or R′COOH, TBTU, TEA, DMF; (c) AcOH, MeOH, DCM; (d) (i) HOBt, resin-bound carbodiimide, DCM, (ii) resin-bound polyamine; (e) TFA.

Table 1. Inhibitory Activities against UPA and Related Enzymes

			IC_{50} (μM) or % inhibition at given concentration[a] (μM)				
	IC_{50} (nM) uPA	k_{app} (M^{-1} s^{-1}) uPA	tPA	plasmin	thrombin	FXa	trypsin
2	61 ± 1	1.77×10^3 $\pm 0.08 \times 10^3$	50% @ 2.5 (~40)	10.8 ± 0.3 (300)	0.50 ± 0.02 (8)	65 ± 4 (1100)	N.D.
3a	4.3 ± 0.2	60×10^3 $\pm 2 \times 10^3$	4.6 ± 0.7 (1000)	2.0 ± 0.2 (470)	20 ± 0.3 (4700)	43% @ 125	0.3 ± 0.1 (70)
3b	2.6 ± 0.3	94×10^3 $\pm 4 \times 10^3$	3.1 ± 0.7 (1200)	1.9 ± 0.1 (740)	4.9 ± 0.3 (1900)	64% @ 250	0.16 ± 0.2 (60)
3c	3.5 ± 0.7	97×10^3 $\pm 7 \times 10^3$	0.28 ± 0.02 (80)	0.037 ± 0.003 (11)	0.77 ± 0.03 (220)	33 ± 5 (9400)	0.31 ± 0.03 (90)
3d	5 ± 1	40×10^3 $\pm 2 \times 10^3$	15 ± 2 (3000)	15 ± 1 (3000)	22 ± 1 (5400)	45% @ 250	0.40 ± 0.05 (80)
3e	5.8 ± 1.2	46×10^3 $\pm 2 \times 10^3$	4.4 ± 0.5 (76o)	0.99 ± 0.05 (155)	6 ± 1 (1000)	96 ± 14 (16 551)	0.280 ± 0.04 (50)
3f	1.5 ± 0.2	80×10^3 $\pm 10 \times 10^3$	3.4 ± 0.1 (2300)	1.54 ± 0.17 (1000)	4.3 ± 0.2 (2800)	68% @ 250	0.098 ± 0.006 (65)
3g	6.9 ± 0.8	71×10^3 $\pm 0.2 \times 10^3$	13 ± 2 (1900)	10 ± 1 (1400)	35 ± 4 (5000)	~250	280 ± 30 (40)
3h	8 ± 1	36×10^3 $\pm 1 \times 10^3$	8.6 ± 0.6 (1000)	5 ± 1 (600)	6 ± 0.1 (750)	62% @ 250	0.16 ± 0.03 (20)
3i	5.8 ± 0.4	98×10^3 $\pm 6 \times 10^3$	4.3 ± 0.2 (740)	1.7 ± 0.3 (293)	1.67 ± 0.04 (288)	100 ± 18 (19 000)	0.36 ± 0.04 (60)
3j	6.6 ± 0.5	45×10^3 $\pm 1 \times 10^3$	3.7 ± 0.2 (560)	0.9 ± 0.1 (136)	2.98 ± 0.03 (451)	58 ± 7 (9000)	0.24 ± 0.02 (36)
3k	6.2 ± 0.3	74×10^3 $\pm 4 \times 10^3$	6.6 ± 0.5 (1100)	0.9 ± 0.2 (145)	7.5 ± 0.4 (1200)	53% @ 250	0.44 ± 0.06 (70)
3l	7 ± 2	70×10^3 $\pm 10 \times 10^3$	16 ± 1 (2300)	5.0 ± 0.4 (700)	67 ± 12 (9600)	53% @ 250	0.16 ± 0.03 (23)
3m	4.4 ± 0.6	75×10^3 $\pm 10 \times 10^3$	18 ± 3 (4000)	8 ± 1 (1800)	34 ± 4 (7700)	56% @ 250	0.16 ± 0.03 (40)
3n	5 ± 1	83×10^3 $\pm 11 \times 10^3$	5.5 ± 0.4 (1100)	7.2 ± 0.5 (1400)	15.9 ± 0.6 (3200)	57% @ 250	0.14 ± 0.02 (30)
3b	6 ± 1	62×10^3 $\pm 7 \times 10^3$	3.6 ± 0.4 (600)	4.2 ± 0.2 (700)	6.3 ± 0.2 (1000)	62% @ 250	0.22 ± 0.06 (40)
4	6.7 ± 0.3	49×10^3 $\pm 1 \times 10^3$	6.4 ± 0.3 (1000)	0.9 ± 0.01 (130)	1.5 ± 0.04 (200)	58% @ 250	0.20 ± 0.04 (30)

[a] Selectivity index is given in parentheses (IC_{50}/IC_{50} uPA).

Scheme 2. Synthesis of the Intermediate **14**

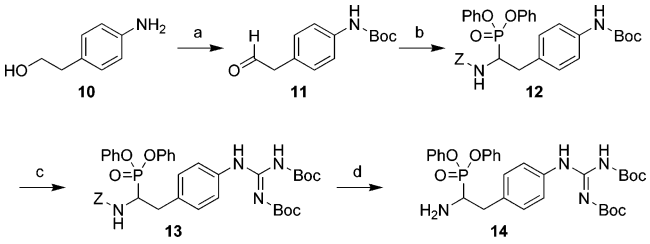

Conditions: (a) (i) di-*tert*-butyl dicarbonate, TEA, dioxane, (ii) Dess−Martin oxidation; (b) benzyl carbamate, triphenyl phosphite, $Cu(OTf)_2$, DCM; (c) (i) TFA, (ii) *N*,*N*′-bis(*tert*-butoxycarbonyl)-1-guanylpyrazole, MeCN; (d) H_2, Pd/C.

The aminophosphonate building block **14** was prepared from *tert*-butylcarbamate-protected 4-aminophenylacetaldehyde (**11**), prepared from the corresponding alcohol (**10**) with Dess−Martin periodinane, as described earlier[15] (Scheme 2). For the amidoalkylation, we used a previously developed procedure with copper triflate as catalyst, affording *N*-benzyloxycarbonyl-protected diphenyl phosphonate **12**.[20] These softer conditions allow the use of Boc protecting groups, which is not possible with the standard acetic acid conditions. Acidolysis removed the *tert*-butyl carbamate protecting group. *N*,*N*′-bis(*tert*-butoxycarbonyl)-1-guanylpyrazole was used to introduce the protected guanidine group. Compound **13** was subsequently deprotected under hydrogenolytic conditions (Scheme 2). The *p*-acetylaminophenyl phosphonate **4** was prepared analogously using tri-*p*-acetylaminophenyl phosphite.[18]

Biochemical Evaluation

The diphenyl phosphonate tripeptides were evaluated for their ability to inhibit various trypsin-like serine proteases using the appropriate chromogenic substrates.[15] The IC_{50} values were determined for uPA and five other exemplatory trypsin-like serine proteases. Four of them are involved in the blood coagulation cascade (tPA, plasmin, thrombin, and FXa; Table 1).

Compound **2** is the original lead diphenyl phosphonate with arginine at P1 showing low activity and limited selectivity.[15] Potency and selectivity is enhanced when the arginine analogue at P1 is replaced with a benzylguanidine group (**3a**). When the terminal benzylcarbamate function (**3a**) was substituted for a sulfonyl or acyl group, all compounds remain equipotent toward uPA with IC_{50} values of about 5 nM but show varying selectivities as a result of enhanced or reduced affinities for plasmin, tPA, thrombin, FXa, and trypsin. We found that amide groups in general and a benzamide group in particular at the P4 position were the most selective compounds (**3d**). Increases in selectivity of 2- to 6-fold were observed compared to that of **3a**. The selectivity index toward trypsin, however, is limited to about 80. Although rather low, this index is still far better than the corresponding index for related peptide-like inhibitors.[15]

Paracetamol ester **4** was found to be a very potent inhibitor of uPA with low nanomolar activity, comparable to the parent compound **3a**. There was, however, a small decrease in selectivity toward plasmin and a significant decrease in selectivity toward thrombin. The selectivity profile of this acetamidophenyl phosphonate **4**, however, can still be considered as promising.

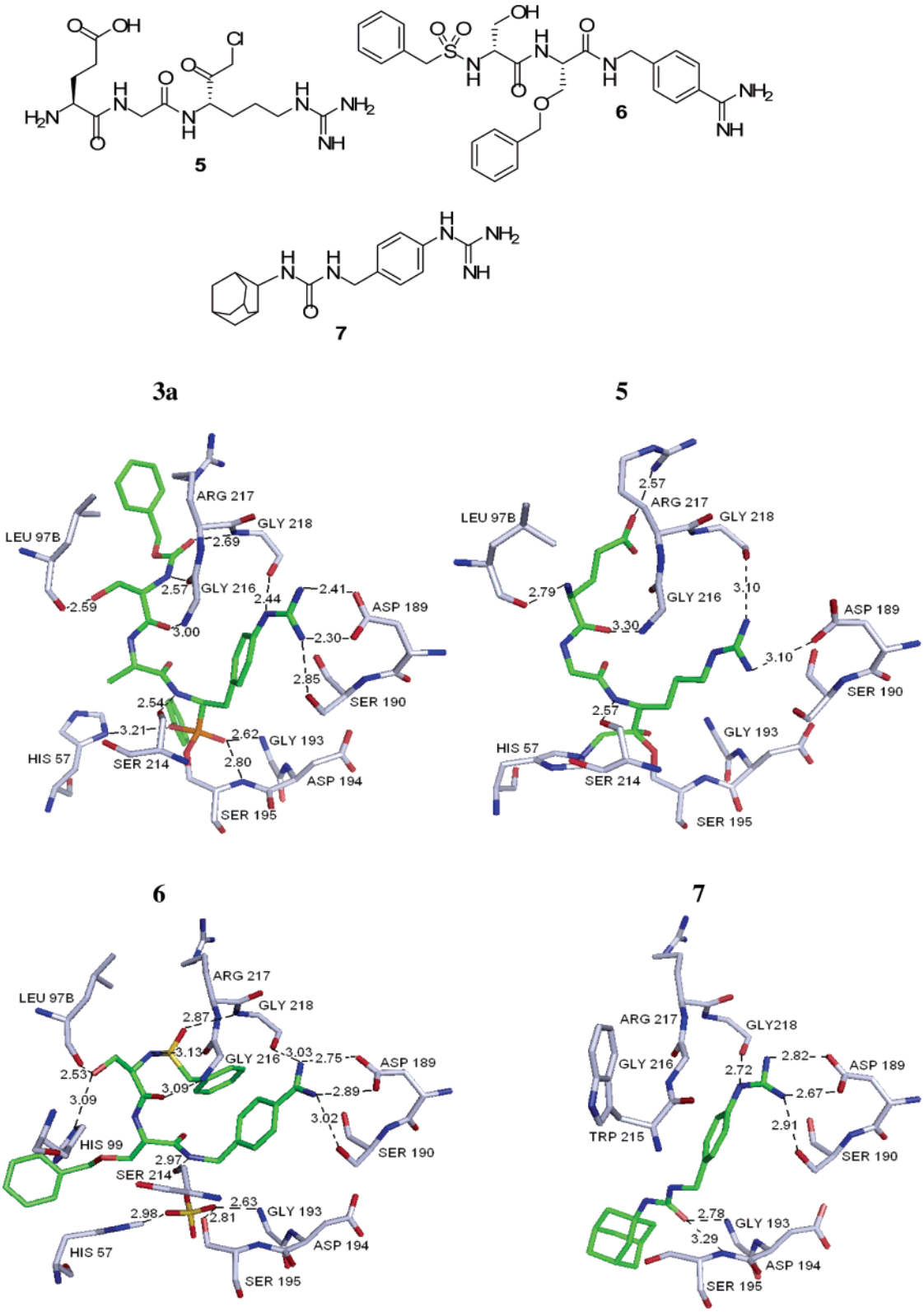

Figure 3. Inhibitors **3a** and **5**−**7** in the active site of uPA with ionic- and hydrogen bonds (carbons of inhibitors, green; carbons of uPA, gray; nitrogen, blue; oxygen, red; sulfur, yellow; phosphorus, orange). Compound **3a** was modeled as a flexible ligand in a flexible uPA pocket.

The hypothesis that these compounds are indeed irreversible inhibitors of uPA is supported by their kinetic behavior. The inhibition was time-dependent and the rate of inactivation increased with the inhibitor concentration. When the reaction was allowed to proceed to completion, the enzyme was fully inhibited, even at nM concentrations. The inactivation rate decreased in the presence of substrate, indicating competition between the inhibitors and the substrate for the enzyme's active site. Lowering the inhibitor concentration by diluting the inhibited enzyme with substrate solution did not cause a rise in uPA activity. We selected compound **4** to evaluate whether it is also an irreversible inhibitor for the other investigated enzymes. Compound **4** showed irreversible binding properties for uPA, tPA, and trypsin. Surprisingly, the slow recovery of

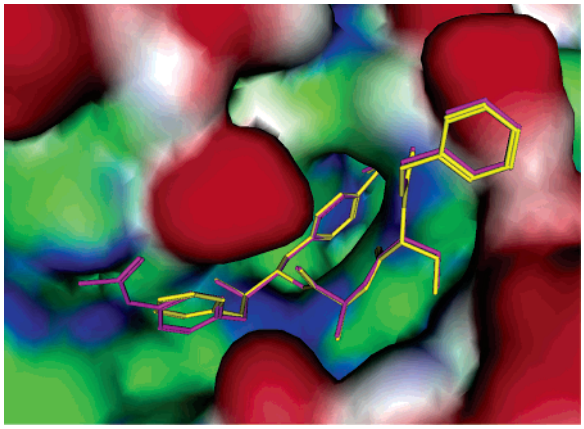

Figure 4. Inhibitors **3a** (yellow) and **4** (pink) shown in the active site of uPA. The molecular surface of uPA is visualized (red = solvent accessible, green = hydrophobic, blue = hydrophilic).

the enzymatic activity of thrombin, after dilution of the preformed enzyme−inhibitor complex, indicated that **4** is either a reversible slow-binding thrombin inhibitor or that the phosphonylated active site serine is hydrolyzing. A similar behavior (but less obvious) was observed with plasmin.

To check the possibility to evaluate our compounds in a mouse model, we tested compound **4** toward the murine enzymes uPA, plasmin, and tPA. The IC_{50} value for muPA is 410 ± 60 nM, and there is only a factor 5 in selectivity toward the two other murine enzymes. These data were in agreement with formerly published results comparing the species specificity of amidine-based urokinase inhibitors.[21] It is known that there is a small but important difference in the sequence of the active site of mouse uPA compared to human uPA. This result shows that it is not beneficial to test these compounds in an all-mouse tumor model.

Molecular Modeling

A molecular modeling study was performed to explain the high potency and remarkable selectivity of the here reported uPA inhibitors. A first question was how compound **3a** fits in the active site of uPA. We decided to model the complex after reaction of the diphenyl phosphonate with the active site serine because we believe this reflects best the transition state of the reaction. However, we were also able to model the diphenyl phosphonate in the active site before the reaction (results not shown).

The model of **3a** in uPA was constructed from the superposition of the crystal structures of three different inhibitors (**5**−**7**), followed by energy minimization.[6,22,23] The benzylguanidine moiety fits nicely in the S1 specificity pocket of uPA (Figure 3). The terminal guanidine forms a symmetrical salt bridge with the carboxylate of Asp189. One nitrogen atom makes a hydrogen bond with the carbonyl oxygen of Gly218, and another nitrogen atom forms a hydrogen bond with Ser190 OH. This Ser190 in the S1 pocket is one of the important specificity factors because it is present in uPA, plasmin, and trypsin but is replaced by Ala190 in tPA, thrombin, and factorXa.[24] The phenyl ring is sandwiched between the planes of the amide bonds of Trp215−Gly216 and Ser190−Cys191 and Tyr228 at the back. Because the synthesized compounds are diastereomeric mixtures at the carbon connected to the phosphorus atom and because the phosphorus atom becomes chiral after covalent linkage with the oxygen of Ser195, we investigated which of the four possible diastereomers gave the best fit in the active site. It turned out that *R*-stereochemistry at the carbon, corresponding to the natural *L*-amino acids, and the *R*-stereochemistry at the phosphorus gave the most plausible result. The phosphonate oxygen is directed toward the oxyanion hole where it forms two hydrogen bonds with the backbone NH groups of Gly193 and Ser195. The phenol oxygen forms a hydrogen bond with the protonated His57 from the catalytic triad. The phenyl ring of the phenol is put into the hydrophobic S1′ pocket. The P2 alanine is placed in the small S2 pocket. The hydroxyl group of the P3 D-Ser interacts with the carbonyl oxygen of Leu97B. Together with Thr97A, the residue Leu97B is part of an uPA-specific insertion loop, which is not present in the other related trypsin-like serine proteases. The CO and NH of the P3 residue form a hydrogen bond with, respectively, the NH and CO of Gly216, and the carbonyl oxygen of the benzyl carbamate forms a hydrogen bond with the backbone NH of Gly218. These contacts compare well with those of the reported crystal structures of **5**−**7** (Figure 3).

The highly specific interactions in the S1 pocket explain why the benzylguanidine inhibitors (**3**) are much more potent than the previously described diphenyl phosphonates.[15] Modeling of the arginine analogue **2** in uPA showed that, when the phosphor atom is covalently linked to Ser195, there is no possibility to form the salt bridge with Asp189. Indeed, the distance between the phosphor atom and the carbon atom of the guanidine is 9.24 Å in **3a** bound to uPA, whereas it is only 7.76 Å in **2** bound to uPA. Similar modeling conclusions could be obtained for the other P1 modifications.[15]

We also studied why compounds **3** are highly selective with respect to the related trypsin-like enzymes. The general order of potency of these compounds toward the studied enzymes is uPA > trypsin > plasmin > tPA > thrombin > FXa. There are several factors that contribute to this selectivity. The first one is the much deeper S1 pocket of uPA. The distance from the side-chain oxygen of Ser195 to the carboxylic carbon atom of Asp189 is about 0.5 Å longer compared to that of trypsin, plasmin, tPA, and FXa and about 0.9 Å longer compared to that of thrombin. These smaller pockets hamper the correct positioning of the benzylguanidine. A second factor is the above-mentioned difference between the Ser190 enzymes (uPA, trypsin, and plasmin) and the Ala190 enzymes (tPA, thrombin, and FXa). The oxygen of the side chain of Ser190 forms an extra hydrogen bond with one of the nitrogens of the guanidine of the inhibitor and explains the higher potency toward the Ser190 enzymes. A third contributing factor is the presence of a unique insertion loop in uPA (Thr97A−Leu97B) forming a hydrogen bond with the hydroxyl of the D-Ser in the inhibitors. Further arguments for the selectivity order can be found in the sequence identity. The overall sequence identity with uPA is highest for tPA (44%), lower for trypsin and plasmin (34%), and lowest for thrombin and FXa (29%). Apart from tPA, this agrees well with the general order of potency. The lower potency for tPA can be explained by the much lower sequence identity with uPA when only the 28 amino acids are considered that have at least one atom within a distance of 4.5 Å of **3a**. This sequence identity is 81 and 74% for trypsin and plasmin, respectively, whereas it is only 59% for tPA.

In several models we noticed the same interactions irrespective of the nature of the P4 substituent, which explains their equal potency toward uPA. Some differences in selectivity are observed, but this could not be explained by our molecular models.

Finally, the diparacetamol phosphonate **4** and the diphenyl phosphonate **3a** are equally potent toward uPA. The pocket accommodating the phenyl or paracetamol is large enough, and

no extra interactions are observed with the *p*-acetylamino group (Figure 4). With respect to the selectivity of **4**, the most significant difference is the 13-fold higher potency of **4** toward thrombin. This can be explained by an extra hydrogen bond between the nitrogen of the *p*-acetylamino group and a carboxylic oxygen of Glu192.

Conclusions

An efficient method to make a small library of potent and highly selective irreversible uPA inhibitors was developed. The best compounds show uPA inhibiting activities of about 5 nM (IC_{50}, 15 min, 37 °C) and remarkable in vitro selectivity indices of 3000 or more toward related enzymes from the fibrinolytic and blood coagulation systems. Compound **3d** belongs to the most potent and selective uPA inhibitors ever reported. We have shown that these diphenyl phosphonates irreversibly inhibit uPA. A potent and selective *p*-acetylaminophenol analogue was developed to circumvent the release of cytotoxic phenol. Differences in potency and selectivity of these inhibitors could be explained by molecular modeling.

Experimental Section

Chemistry. Amino acids and TBTU were purchased from Novabiochem. Other reagents were obtained from Sigma-Aldrich or Acros. Characterization of all compounds was done with ^{1}H NMR and mass spectrometry. ^{1}H NMR spectra were recorded on a 400 MHz Bruker Avance DRX-400 spectrometer. ES Mass spectra were obtained from an Esquire 3000plus iontrap mass spectrometer from Bruker Daltonics. Purity was verified using two diverse HPLC systems using, respectively, a mass and UV detector. Water (A) and ACN (B) were used as eluents. LC-MS spectra were recorded on an Agilent 1100 series HPLC system using an Alltech Prevail C18 column (2.1 × 50 mm, 3 μm) coupled with an Esquire 3000plus as MS detector and a 5−100% B, 20 min gradient was used with a flow rate from 0.2 mL/min. Formic acid (0.1%) was added to solvents A and B. Reversed phase HPLC was run on a Gilson instrument equipped with an Ultrasphere ODS column (4.6 × 250 mm, 5 μm). A 10−100% B, 35 min gradient was used with a flow rate from 1 mL/min. TFA (0.1%) was added to solvents A and B. A 214 nm wavelength was used. When necessary, the products were purified with flash chromatography on a Flashmaster II (Jones Chromatography) with a 30 min gradient of 0−50% EtOAc in hexane or 0−25% MeOH in EtOAc.

4-(*tert*-Butyloxycarbonylamino)phenylacetaldehyde (11). To a solution of the amino alcohol **10** in 40 mL of dioxane were added triethylamine (1 equiv) and di-*tert*-butyl dicarbonate (1.1 equiv). The mixture was stirred at room temperature for 1−8 h (reaction was monitored by TLC). The solution was concentrated in vacuo and acidified with 2 N HCl. The acidified aqueous layer was extracted with EtOAc (3×). The combined organic layers were dried over Na_2SO_4 and evaporated under reduced pressure yielding the Boc-protected *N*-substituted alcohol, which was purified by flash column chromatography (EtOAc/hexane).

To a stirred suspension of this alcohol (1 equiv) in DCM (80 mL) at −78 °C, a solution of Dess−Martin periodane (1.5 equiv from a 15 wt % solution) was added. The suspension was stirred for 3 h at room temperature. The resulting solution was poured into a vigorously stirred saturated $NaHCO_3$ and $Na_2S_2O_3$ solution (1:1/100 mL). The organic layer was separated and washed with brine and dried over Na_2SO_4. The crude aldehyde **11** was obtained by removing the solvent in vacuo and used in the next step without further purification. Yield: 58%. ^{1}H NMR ($CDCl_3$): δ 1.5 (s, 9H), 3.75 (d, 2H), 7.10 (d, 2H), 7.30 (m, 2H), 9.6 (t, 1H). MS (ESI): *m*/*z* 258 [M + Na], 290 [M + MeOH + Na].

Diphenyl 1-Benzyloxycarbonylamino-2-(4-*tert*-butyloxycarbonylaminophenyl)ethanephosphonate (12). To a solution of crude aldehyde **11**, triphenyl phosphite (1 equiv), and benzyl carbamate (1 equiv) in DCM (50 mL), 0.1 equiv $Cu(OTf)_2$ was added. The solution was stirred at room temperature for 4 h. DCM was removed in vacuo. The crude product was dissolved in MeOH, and the solution was kept at 4 °C until precipitation of diphenyl phosphonate was complete. The precipitated product was filtered off and crystallized from MeOH to give **12** as a white solid. Yield: 30%. ^{1}H NMR ($CDCl_3$): δ 1.5 (s, 9H), 3.0−3.5 (m, 2H), 4.7 (m, 1H), 5.1 (m, 2H), 5.2 (d, 1H), 6.5 (s, 1H), 7.1−7.4 (m, 19H). MS (ESI): *m*/*z* 625 [M + Na].

Di-(4-acetamidophenyl)-1-(benzyloxycarbonylamino)-2-(4-*tert*-butyloxycarbonylaminophenyl)ethanephosphonate (Paracetamol Analogue of 12). The procedure as given for **12** was followed, except using tri-4-acetamidophenyl phosphite. The crude product was purified by flash column chromatography (EtOAc/MeOH) to give pure **12** as a white foam. Yield: 20%. ^{1}H NMR (CD_3OD): δ 1.5 (s, 9H), 2.0 (s, 6H), 4.6 (m, 1H), 5.1 (m, 2H), 7.1−7.3 (m, 13H), 7.5 (m, 4H). MS (ESI): *m*/*z* 739 [M + Na].

Diphenyl 1-(Benzyloxycarbonylamino)-2-(4-*N*,*N*′-bis(*tert*-butyloxycarbonyl)guanidino)phenyl)ethanephosphonate (13). The Boc-protected compound **12** was dissolved in 50% TFA in DCM (2−5 mL). After stirring for 3 h at room temperature, the solvent was evaporated. The crude oil was washed with cold ether, and a precipitate was formed. *N*,*N*′-Bis(*tert*-butyloxycarbonyl)-guanidinopyrazole (1 equiv) and TEA (1 equiv) in ACN (5 mL) were added, and the mixture was stirred at reflux temperature overnight. The solvent was evaporated, and the residue was dissolved in EtOAc. The organic layer was washed with 1 N HCl, saturated $NaHCO_3$ solution, and brine. The organic layer was dried with Na_2SO_4 and evaporated. Yield 65%. ^{1}H NMR ($CDCl_3$): δ 1.5 (s (2×), 18H), 3.0−3.4 (m, 2H), 4.7 (m, 1H), 5.1 (m, 2H), 7.1−7.4 (m, 19H). MS (ESI): *m*/*z* 745 [M + Na].

Di-(4-acetamidophenyl) 1-(Benzyloxycarbonylamino)-2-{4-[*N*,*N*′-bis(*tert*-butyloxy-carbonyl)guanidino]phenyl}ethanephosphonate (Paracetamol Analogue of 13). This compound was prepared in the same way as **13** using the corresponding paracetamol analogue of **12**. Yield: 40%. ^{1}H NMR ($CDCl_3$): δ 1.5 (d, 18H), 2.0 (d, 6H), 2.9−3.2 (m, 2H), 4.6 (m, 1H), 5.1 (s, 2H), 6.7−7.3 (m, 17H), 8.7 (s, 1H), 8.8 (s, 1H), 10.2 (s, 1H), 11.7 (s, 1H).

Diphenyl 1-Amino-2-(4-*N*,*N*′-bis(*tert*-butyloxycarbonyl)guanidino)phenyl)ethanephosphonate (14). The *Z*-protected phosphonate (1 equiv) **13** was dissolved in 20 mL MeOH. Pd/C (10%) was added. After removing the oxygen with N_2, H_2 was bubbled through the solution. The solution was stirred for 8 h at room temperature. The solution was filtered over Celite, and the filtrate was evaporated. Compound **14** was used without further purification.

Di(4-acetamidophenyl) 1-Amino-2-(4-*N*,*N*′-bis(*tert*-butyloxycarbonyl)guanidino)phenyl)ethanephosphonate (Paracetamol Analogue of 14). This compound was prepared in the same way as **14** using the corresponding paracetamol analogue of **13**.

Deprotection of the Compounds 9 to the Final Compounds 3. Compounds **9** were dissolved in 50% TFA in DCM (2−5 mL). After stirring for 3 h at room temperature, the solvent was evaporated. The crude oil was washed with cold ether, and a precipitate was formed.

Diphenyl 1-[(*N*-Benzoyloxycarbonyl-D-seryl)-L-alanyl]amino-2-(4-guanidinophenyl)ethanephosphonate Trifluoroacetate (3a). Yield: 85%. ^{1}H NMR ($CDCl_3$): δ 1.3 (m, 3H), 3.0−3.4 (m, 2H), 3.6 (m, 2H), 4.25 (m, 1H), 4.4 (m, 1H), 5.1 (m, 3H), 7.1−7.4 (m, 19H). HPLC: 214 nm, t_r 19.98 min, 100%. LC/MS: t_r 14.4 min, 100%. MS (ESI): *m*/*z* 703 (M^{+1}).

Diphenyl 1-[(*N*-Benzenesulfonyl-D-seryl)-L-alanyl]amino-2-(4-guanidinophenyl)ethanephosphonate Trifluoroacetate (3b). Yield: 71%. ^{1}H NMR (CD_3OD): δ 1.1 (m, 3H), 3.0 (m, 2H), 3.6 (m, 2H), 4.0 (m, $0.5H_A$), 4.1 (m, $0.5H_B$), 4.9 (m, $0.5H_A$), 5.1 (m, $0.5H_B$), 7.0−7.8 (m, 19H). HPLC: 214 nm, t_r 19.24 min, 97.27%; 254 nm, t_r 19.30 min, 100%. LC/MS: t_r 13.0 min, 100%. MS (ESI): *m*/*z* 709 [M + Na].

Diphenyl 1-[(*N*-α-Toluenesulfonyl-D-seryl)-L-alanyl]amino-2-(4-guanidinophenyl)ethanephosphonate Trifluoroacetate (3c). Yield: 76%. ^{1}H NMR (CD_3OD): δ 1.1 (d, 3H), 3.0 (m, 1H), 3.2−3.5 (m, 3H), 3.6 (s, 2H), 3.7 (m, 1H), 4.1 (m, 1H), 4.9 (m, $0.5H_A$), 5.1 (m, $0.5H_B$), 7.0−7.4 (m, 19H). HPLC: 214 nm, t_r 19.54 min,

100%; 254 nm, t_r 19.56 min, 100%. LC/MS: t_r 13.3 min, 93.5%. MS (ESI): *m*/*z* 723 [M + Na].

Diphenyl 1-[(*N*-Benzyl-D-seryl)-L-alanyl]amino-2-(4-guanidinophenyl)ethanephosphonate Trifluoroacetate (3d). Yield: 46%. ^{1}H NMR (CD_3OD): δ 1.3 (d, 3H), 3.3 (d, 1H), 3.5 (m, 1H), 4 (m, 2H), 4.2 (2m, 1H), 4.5 (dm, 1H), 7.0−7.6 (m, 19H). HPLC: 214 nm, t_r 18.12 min, 46.90%; t_r 17.72 min, 43.45%; 254 nm, t_r 17.99 min, 48.69%; t_r 17.59 min, 42.39%. LC/MS: t_r 12.7 min, 99.9%. MS (ESI): *m*/*z* 695 [M + Na].

Diphenyl 1-[(*N*-Naftalenesulfonyl-D-seryl)-L-alanyl]amino-2-(4-guanidinophenyl)ethanephosphonate Trifluoroacetate (3e). Yield: 55%. ^{1}H NMR (CD_3OD): δ 1.0 (d, 3H), 3.2 (m, 1H), 3.5 (m, 2H), 3.6−3.8 (dm, 2H), 4.1 (dm, 1H), 5.0 (m, 1H), 7.0−7.7 (m, 18 H), 8.0 (m, 1H), 8.1 (m, 1H), 8.3 (d, 1H), 8.7 (m, 1H). HPLC: 214 nm, t_r 20.20 min, 100%; 254 nm, t_r 20.13 min, 100%. LC/MS: t_r 14.4 min, 97.7%. MS (ESI): *m*/*z* 781 [M + Na].

Diphenyl 1-[(*N*-2-Thiophenesulfonyl-D-seryl)-L-alanyl]amino-2-(4-guanidinophenyl)ethanephosphonate Trifluoroacetate (3f). Yield: 35%. ^{1}H NMR ($CDCl_3$): δ 1.3 (m, 3H), 3.1 (m, 1H), 3.4 (m, 1H), 3.6 (m, 2H), 3.9 (m, 1H), 4.25 (m, 1H), 4.4 (m, 1H), 7.1−7.4 (m, 15H), 7.6 (m, 1H), 7.7 (m, 1H). HPLC: 214 nm, t_r 18.62 min, 100%. HPLC: 254 nm, t_r 18.23 min, 100%. LC/MS: t_r 12.9 min, 94.9%. MS (ESI): *m*/*z* 715 (M^{+1}).

Diphenyl 1-[(*N*-2-Thienyl-D-seryl)-L-alanyl]amino-2-(4-guanidinophenyl)ethanephosphonate Trifluoroacetate (3g). Yield: 55%. ^{1}H NMR ($CDCl_3$): δ 1.3 (m, 3H), 3.4 (m, 2H), 3.9 (m, 2H), 4.2−4.3 (m, 2H), 5.1 (m, 1H), 7.1−7.8 (m, 17H). HPLC: 214 nm, t_r 17.02 min, 42.13%; 17.50 min, 57.87%. HPLC: 254 nm, t_r 16.89 min, 41.55%; 17.45 min, 58.45%. LC/MS: t_r 12.9 min, 94.9%. MS (ESI): *m*/*z* 679 (M^{+1}).

Diphenyl 1-[(*N*-1-Adamantanyl-D-seryl)-L-alanyl])amino-2-(4-guanidinophenyl)ethanephosphonate Trifluoroacetate (3h). Yield: 67%. ^{1}H NMR ($CDCl_3$): δ 1.28 (dd, J = 8.4 and J = 16, 1H), 1.30 (dd, J = 8.4 and J = 16), 1.7 (m, 6H), 1.9 (m, 5H), 2.0 (m, 4H), 3.25 (m, 1H), 3.45 (m, 1H), 3.75 (m, 2H), 4.1 (m, 1H), 4.3 (m, 1H), 5.1 (m, 1H), 7.0−7.9 (m, 14H). HPLC: 214 nm, t_r 19.96 min, 77.42%; 254 nm, t_r 20.89 min, 35.77%; 21.22 min, 38.96%. LC/MS: t_r 13.9 min, 98.8%. MS (ESI): *m*/*z* 731 (M^{+1}).

Diphenyl 1-[(*N*-*p*-Methoxybenzenesulfonyl-D-seryl)-L-alanyl]-amino-2-(4-guanidinophenyl)ethane-phosphonate Trifluoroacetate (3i). Yield: 23%. ^{1}H NMR (CD_3OD): δ 1.2 (m, 3H), 3.1 (m, 1H), 3.4 (m, 3H), 3.5−3.6 (m, 2H), 3.8 (m, 2H), 4.0 (m, 1H), 4.2 (m, 1H), 5.1 (m, 1H), 7.0−8.0 (m, 18H). HPLC: 214 nm, t_r 19.62 min, 100%; 254 nm, t_r 19.23 min, 100%. LC/MS: t_r 13.8 min, 94.9%. MS (ESI): *m*/*z* 761 [M + Na].

Diphenyl 1-[(*N*-*p*-Bromobenzenesulfonyl-D-seryl)-L-alanyl]-amino-2-(4-guanidinophenyl)ethane-phosphonate Trifluoroacetate (3j). Yield: 55%. ^{1}H NMR ($CDCl_3$): δ 1.2 (m, 3H), 3.1 (m, 1H), 3.2 (s, 2H), 3.5 (m, 1H), 3.6−3.7 (dm, 2H), 4.2 (m, 2H), 7.0−8.0 (m, 18H). HPLC: 214 nm, t_r 21.09 min, 94.07%; 254 nm, t_r 20.10 min, 94.61%. LC/MS: t_r 14.1 min, 96.4%. MS (ESI): *m*/*z* 809 [M + Na].

Diphenyl 1-[(*N*-*p*-Cyanobenzenesulfonyl-D-seryl)-L-alanyl]-amino-2-(4-guanidinophenyl)ethane-phosphonate Trifluoroacetate (3k). Yield: 43%. ^{1}H NMR (CD_3OD): δ 1.3 (d, 3H), 3.2 (m, 1H), 3.5 (m, 2H), 3.6−3.9 (dm, 2H), 4.2 (m, 1H), 5.1 (m, 1H), 7.1−7.4 (dm, 14H), 7.8−8.0 (dm, 4H). HPLC: 214 nm, t_r 18.86 min, 92.64%; 254 nm, t_r 18.79 min, 95.59%. LC/MS: t_r 13.1 min, 100%. MS (ESI): *m*/*z* 757 [M + Na].

Diphenyl 1-[(*N*-*p*-Methylbenzoyl-D-seryl)-L-alanyl]amino-2-(4-guanidinophenyl)ethanephosphonate Trifluoroacetate (3l). Yield: 93%. ^{1}H NMR ($CDCl_3$): δ 1.28 (dd, J = 2.8 and J = 7.2, 1H), 1.30 (dd, J = 2.4 and J = 7.2), 2.38 (d, 3H), 3.25 (m, 1H), 3.45 (m, 1H), 3.85 (dd, J = 5.6 and J = 14.8, 1H), 3.92 (dd, J = 5.6 and J = 14.8, 1H), 4.2 (m, 0.5H), 4.35 (m, 0.5H), 4.45 (m, 0.5H), 4.53 (m, 0.5H), 5.1 (m, 1H), 7.0−7.9 (m, 18H). HPLC: 214 nm, t_r 18.46 min, 47.58%; t_r 18.82 min, 44.80%. HPLC: 254 nm, t_r 18.59 min, 47.64%; t_r 19.04 min, 43.96%. LC/MS: t_r 13.4 min, 100%. MS (ESI): *m*/*z* 687 (M^{+1}).

Diphenyl 1-[(*N*-*o*-Methylbenzoyl-D-seryl)-L-alanyl]amino-2-(4-guanidinophenyl)ethanephosphonate Trifluoroacetate (3m). Yield: 92%. ^{1}H NMR ($CDCl_3$): δ 1.26 (dd, J = 2.4 and J = 7.2, 1H), 1.28 (dd, J = 2.4 and J = 7.2), 2.4 (s, 3H), 3.2 (m, 1H), 3.4 (m, 1H), 3.8 (m, 2H), 4.25 (m, 1H), 4.4 (m, 1H), 5.1 (m, 1H), 7.0−7.9 (m, 18H). HPLC: 214 nm, t_r 18.56 min, 100%. HPLC: 254 nm, t_r 18.56 min, 46.32%, t_r 19.00 min, 46.32%. LC/MS: t_r 13.5 min, 100%. MS (ESI): *m*/*z* 687 (M^{+1}).

Diphenyl 1-[(*N*-*o*-Methylbenzoyl-D-seryl)-L-alanyl]amino-2-(4-guanidinophenyl)ethanephosphonate Trifluoroacetate (3n). Yield: 91%. ^{1}H NMR ($CDCl_3$): δ 1.28 (dd, J = 4.4 and J = 7.2, 1H), 1.30 (dd, J = 4.4 and J = 7.2), 2.4 (m, 3H), 3.25 (m, 1H), 3.45 (m, 1H), 3.85 (dd, J = 5.2 and J = 21.2, 1H), 3.92 (dd, J = 5.2 and J = 21.2, 1H), 4.3 (m, 1H), 4.45 (m, 0.5H), 4.52 (m, 0.5H), 5.1 (m, 1H), 7.0−7.9 (m, 18H). HPLC: 214 nm, t_r 18.46 min, 43.41%; t_r 18.82 min, 43.81%; 254 nm, t_r 18.80 min, 40.74%; t_r 19.04 min, 39.77%. LC/MS: t_r 13.6 min, 100%. MS (ESI): *m*/*z* 687 (M^{+1}).

Diphenyl 1-[(*N*-*o*,*o*-Dimethylbenzoyl-D-seryl)-L-alanyl]amino-2-(4-guanidinophenyl)ethanephosphonate Trifluoroacetate (3o). Yield: 94%. ^{1}H NMR ($CDCl_3$): δ 1.28 (dd, J = 7.2 and J = 12.4, 1H), 1.30 (dd, J = 7.2 and J = 12.4), 2.28 (s, 3H), 2.31 (s, 3H), 3.25 (m, 1H), 3.45 (m, 1H), 3.82 (dd, J = 6.4 and J = 21.2, 1H), 3.88 (dd, J = 6.4 and J = 21.2, 1H), 4.3 (m, 1H), 4.55 (m, 0.5H), 4.58 (m, 0.5H), 5.1 (m, 1H), 7.0−7.9 (m, 17H). HPLC: 214 nm, t_r 18.97 min, 39.36%; t_r 19.13 min, 39.54%; 254 nm, t_r 19.00 min, 39.78%; t_r 19.20 min, 38.64%. LC/MS: t_r 13.7 min, 100%. MS (ESI): *m*/*z* 701 (M^{+1}).

Di-(4-acetamidophenyl) 1-[(*N*-Benzyloxycarbonyl-D-seryl)-L-alanyl]amino-2-[4-(guanidino)phenyl]- ethanephosphonate Trifluoroacetate (4). Yield: 93%. ^{1}H NMR ($CDCl_3$): δ 1.3 (m, 3H), 2.0 (s, 6H), 3.0−3.4 (m, 2H), 3.7 (m, 2H), 4.1−4.4 (m, 2H), 5.0 (m, 1H), 5.1 (m, 2H), 7.1−7.6 (m, 17H). HPLC: 214 nm, t_r 14.3 min, 42.1%; t_r 14.0 min, 44.3%. HPLC: 254 nm, t_r 13.8 min, 45.1%; t_r 14.0 min, 49.0%. LC/MS: t_r 12.0 min. Purity: 92.0%. MS (ESI): *m*/*z* 817 (M^{+1}).

uPA Inhibition: in Vitro Evaluation. Enzymatic activity was measured at 37 °C in a Spectramax 340 (Molecular Devices) microtiter plate reader using the chromogenic substrate S-2444 (L-pyroGlu-Gly-L-Arg-*p*-NA·HCl), with a K_m of 80 μM. The substrate was obtained from Chromogenix. The human enzyme was obtained from Sigma-Aldrich and the mouse uPA was obtained from Molecular Innovations, Inc. (U.S.A.). The reaction was monitored at 405 nm, and the initial rate was determined between 0 and 0.25 absorbance units in 20 min. The reaction mixture contained 250 μM substrate and approximately 1 mU of enzyme in 145 μL of buffer in a final volume of 200 μL. A 50 mM Tris buffer, pH 8.8, was used. From each inhibitor concentration, 5 μL was added, obtaining a final concentration from 0 to 250 μM in a total volume of 0.2 mL. Activity measurements were routinely performed in duplicate. The IC_{50} value is defined as the concentration of inhibitor required to reduce the enzyme activity to 50% after a 15-min preincubation with the enzyme at 37 °C before addition of the substrate. IC_{50} values were obtained by fitting the data with the four-parameter logistics equation using Grafit 5.

$$v = (v\ \text{range})/(1 + \exp(s \times \ln(\text{abs}(I_0/\text{IC}_{50})))) + \text{background}$$

where s = slope factor, v = rate, I_0 = inhibitor concentration, and range = the fitted uninhibited value minus the background. The equation assumes the y falls with increasing x.

Inhibitor stock solutions were prepared in DMSO and stored at −20 °C. Because the compounds described in this paper completely inactivate uPA following pseudo-first-order kinetics, the IC_{50} value is inversely correlated with the second-order rate constant of inactivation. For a simple pseudo-first-order inactivation process, the activity after incubation with inhibitor (v_i) varies with the inhibitor concentration (i), as described in the following equation: $v_i = v_0 \cdot e^{-kit}$, where v_0 is the activity in absence of inhibitor, k is the second-order rate constant of inactivation, and t is the time.

The inactivation rate constant was determined from the time course of inhibition.

The inhibitor was mixed with the substrate (250 μM final concentration), and the buffer solution with the enzyme was added at the time zero. The inhibitor concentrations were chosen to obtain total inhibition of the enzyme within 20 min. The progress curves show the absorbance of *p*-nitroanilide produced as a function of time. Initially, no inhibitor is bound to the enzyme, and the tangent to the progress curve (dA/dt) is proportional to the concentration of the free enzyme. The concentration of free enzyme decreases over time due to the kinetics of inhibitor binding, as described above. Progress curves were recorded in pseudo-first-order conditions ($[I]_0 \gg [E]_0$) and with less than 10% conversion of the substrate during the entire time course. In these conditions, dA/dt decreases exponentially with time. The progress curves were fitted with the integrated rate equation to yield a value for k_{obs}, a pseudo-first-order rate constant.

$$A_t = v_0[1 - \exp(-k_{obs}t)]/k_{obs} + A_0$$

where A_t = absorbance at time t, A_0 = absorbance at time zero, and v_0 = uninhibited initial rate.

The apparent second-order rate constant (k_{app}) was calculated from the slope of the linear part of the plot of k_{obs} versus the inhibitor concentration ($[I]_0$). In case of competition between the inhibitor and the substrate, k_{app} is smaller than the "real" second-order rate constant k discussed above because a certain fraction of the enzyme is present as an enzyme−substrate complex. k_{app} depends on the substrate concentration used in the experiment, as described by Lambeir et al.[25]

Determination of the Selectivity for uPA. The IC_{50} values for plasmin (from human plasma, Sigma), tPA (recombinant, Boehringer Ingelheim), thrombin (from human plasma, Sigma), FXa, and trypsin (bovine, Roche) were determined in the same way as for uPA. S-2288 (H-D-Ile-Pro-Arg-pNa·2HCl) for tPA (K_m: 1 mM), S-2366 (pyroGlu-Pro-Arg-pNA·HCl) for plasmin (K_m: 400 μM) and thrombin (K_m: 150 μM), and S-2772 (Boc-D-Arg-Gly-Arg-pNA·2HCl) for FXa (K_m: 1.5 mM) and BAPNA (Nα-benzoyl-D,L-Arg-pNA·HCl) for trypsin (K_m: 1mM) were used as substrates. FX (Sigma) is activated with Russel's viper venom (Sigma).

The mixture contained 580 μM substrate for thrombin and plasmin, 1.25 mM for tPA, 522 μM for FXa, and 425 μM for trypsin and approximately 5 mU of enzyme and 145 μL of buffer. For tPA and thrombin, Tris buffer, pH 8.3, was used, for FXa, Tris buffer, pH 8.3, with 2.5 mM $CaCl_2$ was used, for plasmin, Tris buffer, pH 7.4, was used, and for trypsin, Tris buffer, pH 8.2, was used. The selectivity index was calculated as (IC_{50} enzyme X)/IC_{50} uPA, where X is tPA, thrombin, plasmin, FXa, or trypsin.

Determination of the Inhibition Type. To follow the dissociation of the inhibitor−enzyme complex, aliquots of enzyme were incubated without inhibitor and in the presence of a concentration of the inhibitor 50 times the IC_{50} at 37 °C. The enzyme concentration was 2.5 times higher than the concentration used for the IC_{50} determinations. After 15 min, the aliquots were diluted 50-fold into the substrate concentration and assay buffer used for the IC_{50} determination. The dissociation of the enzyme−inhibitor complex was monitored by substrate hydrolysis by measuring the absorbance every 20 s.

Molecular Modeling. The molecular modeling studies were performed using MOE 2005.06 software (Chemical Computing Group). All software necessary to build compounds and perform minimizations, alignments, and superpositions is available in the MOE package and was used with standard settings, unless otherwise mentioned. Crystal structures were downloaded from the Protein Databank (PDB), and the ligands were checked and corrected when necessary. Residues not belonging to the enzyme or ligand were removed, including water molecules. Hydrogen atoms were added and energy minimized with MMFF94x force field (standard parameters), keeping all heavy atoms fixed. The following PDB structures of uPA were used: 1VJ9 (**6**), 1LMW (**5**), and 1EJN (**7**). The latter two were aligned and superposed on the first. Compound **3c** was built using different parts of the three ligands in the three mentioned enzymes, followed by covalent linkage to the side-chain oxygen of Ser195. Then the complex was minimized using MMFF94x force field with a flexible ligand in a rigid enzyme. This was followed by minimization using MMFF94x force field of a flexible ligand in a flexible enzyme pocket. This pocket was defined as the amino acids with at least one atom within a distance of 6 Å of the ligand. All other inhibitors were built from **3c**, followed by analogous minimization. The following PDB files were used to study the selectivity toward related enzymes: tPA (1A5H, 1RTF), thrombin (1DWB, 1GJ4, 1H8I), plasmin (1BUI), FXa (1FAX, 1KYE, 1MQ6), and trypsin (1H4W, 1EB2, 1MAX).

Acknowledgment. This work received support from the Fund for Scientific Research-Flanders (Belgium; FWO). P.V. is a postdoctoral fellow of the FWO and G.S. is a visiting postdoc of the FWO. J.J. is a fellow of the Institute of Promotion of Innovation in Science and Technology of Flanders (IWT). The excellent technical assistance of W. Bollaert is greatly appreciated.

Supporting Information Available: Experimental details for the intermediates **8** and **9**, extra modeling pictures, figures demonstrating irreversible inhibition, and purity data for target compounds. This material is available free of charge via the Internet at http://pubs.acs.org.

References

(1) Dano, K.; Behrendt, N.; Hoyer-Hansen, G.; Johnsen, M.; Lund, L. R.; Ploug, M.; Romer, J. Plasminogen Activation and Cancer. *Thromb. Haemostasis* **2005**, *93*, 676−681.
(2) Mazzieri, R.; Blasi, F. The Urokinase Receptor and the Regulation of Cell Proliferation. *Thromb. Haemostasis* **2005**, *93*, 641−646.
(3) Duffy, M. J. The Urokinase Plasminogen Activator System: Role in Malignancy. *Curr. Pharm. Des.* **2004**, *10*, 39−49.
(4) Lee, M.; Fridman, R.; Mobashery, S. Extracellular Proteases As Targets for Treatment of Cancer Metastases. *Chem. Soc. Rev.* **2004**, *33*, 401−409.
(5) Setyono-Han, B.; Sturzebecher, J.; Schmalix, W. A.; Muehlenweg, B.; Sieuwerts, A. M.; Timmermans, M.; Magdolen, V.; Schmitt, M.; Klijn, J. G. M.; Foekens, J. A. Suppression of Rat Breast Cancer Metastasis and Reduction of Primary Tumour Growth by the Small Synthetic Urokinase Inhibitor WX-UKI. *Thromb. Haemostasis* **2005**, *93*, 779−786.
(6) Schweinitz, A.; Steinmetzer, T.; Banke, I. J.; Arlt, M. J. E.; Sturzebecher, A.; Schuster, O.; Geissler, A.; Giersiefen, H.; Zeslawska, E.; Jacob, U.; Kruger, A.; Sturzebecher, J. Design of Novel and Selective Inhibitors of Urokinase-Type Plasminogen Activator With Improved Pharmacokinetic Properties for Use As Antimetastatic Agents. *J. Biol. Chem.* **2004**, *279*, 33613−33622.
(7) Almholt, K.; Lund, L. R.; Rygaard, J.; Nielsen, B. S.; Dano, K.; Romer, J.; Johnsen, M. Reduced Metastasis of Transgenic Mammary Cancer in Urokinase-Deficient Mice. *Int. J. Cancer* **2005**, *113*, 525−532.
(8) Ahmed, N.; Oliva, K.; Wang, Y.; Quinn, M.; Rice, G. Downregulation of Urokinase Plasminogen Activator Receptor Expression Inhibits Erk Signaling With Concomitant Suppression of Invasiveness Due to Loss of UPAR-Beta 1 Integrin Complex in Colon Cancer Cells. *Br. J. Cancer* **2003**, *89*, 374−384.
(9) D'Alessio, S.; Margheri, F.; Pucci, M.; Del Rosso, A.; Monia, B. P.; Bologna, M.; Leonetti, C.; Scarsella, M.; Zupi, G.; Fibbi, G.; Del Rosso, M. Antisense Oligodeoxynucleotides for Urokinase-Plasminogen Activator Receptor Have Anti-Invasive and Anti-Proliferative Effects in Vitro and Inhibit Spontaneous Metastases of Human Melanoma in Mice. *Int. J. Cancer* **2004**, *110*, 125−133.
(10) Margheri, F.; D'Alessio, S.; Serrati, S.; Pucci, M.; Annunziato, F.; Cosmi, L.; Liotta, F.; Angeli, R.; Angelucci, A.; Gravina, G. L.; Rucci, N.; Bologna, M.; Teti, A.; Monia, B.; Fibbi, G.; Del Rosso, M. Effects of Blocking Urokinase Receptor Signaling by Antisense Oligonucleotides in a Mouse Model of Experimental Prostate Cancer Bone Metastases. *Gene Ther.* **2005**, *12*, 702−714.
(11) Weigelt, B.; Peterse, J. L.; van't Veer, L. J. Breast Cancer Metastasis: Markers and Models. *Nat. Rev. Cancer* **2005**, *5*, 591−602.
(12) Rockway, T. W.; Nienaber, V.; Giranda, V. L. Inhibitors of the Protease Domain of Urokinase-Type Plasminogen Activator. *Curr. Pharm. Des.* **2002**, *8*, 2541−2558.
(13) Mackman, R. L.; Katz, B. A.; Breitenbucher, J. G.; Hui, H. C.; Verner, E.; Luong, C.; Liu, L.; Sprengeler, P. A. Exploiting Subsite S1 of Trypsin-Like Serine Proteases for Selectivity: Potent and Selective Inhibitors of Urokinase-Type Plasminogen Activator. *J. Med. Chem.* **2001**, *44*, 3856−3871.

(14) Zeslawska, E.; Jacob, U.; Schweinitz, A.; Coombs, G.; Bode, W.; Madison, E. Crystals of Urokinase Type Plasminogen Activator Complexes Reveal the Binding Mode of Peptidomimetic Inhibitors. *J. Mol. Biol.* **2003**, *328*, 109−118.
(15) Joossens, J.; Van der Veken, P.; Lambeir, A. M.; Augustyns, K.; Haemers, A. Development of Irreversible Diphenyl Phosphonate Inhibitors for Urokinase Plasminogen Activator. *J. Med. Chem.* **2004**, *47*, 2411−2413.
(16) Tamura, S. Y.; Weinhouse, M. I.; Roberts, C. A.; Goldman, E. A.; Masukawa, K.; Anderson, S. M.; Cohen, C. R.; Bradbury, A. E.; Bernardino, V. T.; Dixon, S. A.; Ma, M. G.; Nolan, T. G.; Brunck, T. K. Synthesis and Biological Activity of Peptidyl Aldehyde Urokinase Inhibitors. *Bioorg. Med. Chem. Lett.* **2000**, *10*, 983−987.
(17) Oleksyszyn, J.; Boduszek, B.; Kam, C. M.; Powers, J. C. Novel Amidine-Containing Peptidyl Phosphonates As Irreversible Inhibitors for Blood-Coagulation and Related Serine Proteases. *J. Med. Chem.* **1994**, *37*, 226−231.
(18) Belyaev, A.; Zhang, X. M.; Augustyns, K.; Lambeir, A. M.; De Meester, I.; Vedernikova, I.; Scharpe, S.; Haemers, A. Structure−Activity Relationship of Diaryl Phosphonate Esters As Potent Irreversible Dipeptidyl Peptidase IV Inhibitors. *J. Med. Chem.* **1999**, *42*, 1041−1052.
(19) Senten, K.; Daniels, L.; Van der Veken, P.; De Mester, I.; Lambeir, A. M.; Scharpe, S.; Haemers, A.; Augustyns, K. Rapid Parallel Synthesis of Dipeptide Diphenyl Phosphonate Esters As Inhibitors of Dipeptidyl Peptidases. *J. Comb. Chem.* **2003**, *5*, 336−344.
(20) Van der Veken, P.; El Sayed, I.; Joossens, J.; Stevens, C. V.; Augustyns, K.; Haemers, A. Lewis Acid-Catalyzed Synthesis of *N*-Protected Diphenyl 1-Aminoalkylphosphonates. *Synthesis* **2005**, 634−638.
(21) Klinghofer, V.; Stewart, K.; McGonigal, T.; Smith, R.; Sarthy, A.; Nienaber, V.; Butler, C.; Dorwin, S.; Richardson, P.; Weitzberg, M.; Wendt, M.; Rockway, T.; Zhao, X. M.; Hulkower, K. I.; Giranda, V. L. Species Specificity of Amidine-Based Urokinase Inhibitors. *Biochim. Biophys. Acta* **2001**, *40*, 9125−9131.
(22) Spraggon, G.; Phillips, C.; Nowak, U. K.; Ponting, C. P.; Saunders, D.; Dobson, C. M.; Stuart, D. I.; Jones, E. Y. The Crystal Structure of the Catalytic Domain of Human Urokinase-Type Plasminogen-Activator. *Structure* **1995**, *3*, 681−691.
(23) Sperl, S.; Jacob, U.; de Prada, N. A.; Sturzebecher, J.; Wilhelm, O. G.; Bode, W.; Magdolen, V.; Huber, R.; Moroder, L. (4-Aminomethyl)Phenylguanidine Derivatives As Nonpeptidic Highly Selective Inhibitors of Human Urokinase. *Proc. Natl. Acad. Sci. U.S.A.* **2000**, *97*, 5113−5118.
(24) Katz, B. A.; Mackman, R.; Luong, C.; Radika, K.; Martelli, A.; Sprengeler, P. A.; Wang, J.; Chan, H. D.; Wong, L. Structural Basis for Selectivity of a Small Molecule, S1−Binding, Submicromolar Inhibitor of Urokinase-Type Plasminogen Activator. *Chem. Biol.* **2000**, *7*, 299−312.
(25) Lambeir, A. M.; Borloo, M.; DeMeester, I.; Belyaev, A.; Augustyns, K.; Hendriks, D.; Scharpe, S.; Haemers, A. Dipeptide-Derived Diphenyl Phosphonate Esters: Mechanism-Based Inhibitors of Dipeptidyl Peptidase IV. *Biochim. Biophys. Acta* **1996**, *1290*, 76−82.

JM060622G